Stabilization against ionization via high-Rydberg states

A. Wójcik, R. Parzyński, and A. Grudka
Quantum Electronics Laboratory, Institute of Physics, A. Mickiewicz University, Umultowska 85, 61-614 Poznań, Poland
(Received 18 July 1996; revised manuscript received 30 September 1996)

An analytical study is presented of two models of intense-laser ionization from an isolated initial state via a band of high-Rydberg states in a system which bears many features of the hydrogen atom. The models differ in the way the population from the directly excited Rydberg states can migrate to the states of higher angular momenta. In one of them it migrates via nonresonant and in the other via resonant degenerate Raman coupling. Within these models we draw conclusions about the efficiency of migration, the initial-state lifetime, the redistribution of population, the laser intensities stabilizing the atom against ionization, the effect of the initial state on the threshold stabilizing intensity, as well as about stabilizing mechanisms versus the initial-state choice. [S1050-2947(97)03202-2]

PACS number(s): 42.50.Hz, 32.80.Rm

I. INTRODUCTION

One of the most intriguing phenomena in the current high-intensity laser-atom physics is stabilization of the atom against ionization [1]. With the recent experiment of de Boer *et al.*[2] this phenomenon has left the phase of theoretical predictions and speculations. In this experiment, stabilization was observed in the ionization of the circular $5g$ neon state with a single-photon energy being nearly four times the electron binding energy. Thus the photon energy fulfilled what is usually referred to as the high-frequency condition [3]. Under this condition the measured stabilizing intensities (several times $10^{13}\mathrm{W/cm}^2$ in a 100-fs pulse) were found to be in conformity with the recent calculations of Potvliege and Smith for hydrogen [4]. In the high-frequency ionization, like the measured one, stabilization is determined by the initial-state evolution only and transitions to other bound states do not play a role. This is quite opposite to what takes place in ionization by low frequencies (i.e., the below-ionization-threshold frequencies), the process we shall study within a model hydrogen atom in the present paper.

Precisely, we shall study nominal two-photon ionization from an isolated initial state by light of a frequency ensuring a band of high-Rydberg states to be an intermediary in the transition to the continuum. The inclusion of transition via high-Rydberg states is what makes our paper different from the recent ones [5–8]. The other difference is that we describe the whole process within an analytically solvable model. Such an approximate analytical solution of the problem was possible only under appropriate modeling of the band of highly excited Rydberg states and the couplings between the states of the model. The present model is an essential generalization of two recent analytical models, one proposed by Ivanov [9] and the other by Wójcik and Parzyński [10], and the conclusions drawn from it are based on realistically calculated, representative atom-field coupling parameters. The generalization consists in the inclusion of both nonresonant and resonant Raman-like migration of population from the directly excited band of high-Rydberg states to Rydberg states of higher-angular-momentum quantum number. We included the above-mentioned migration since it was shown to be essential in the related processes (transfer of population from the prepared low-l state to higher-l states of the same principal quantum number $n=28$ in hydrogen [11], the hydrogen $2s$-state two-photon ionization via the low $8p$ Rydberg state [7]). Within the model, we derive analytical solutions for laser pulses shorter in duration than the representative Kepler period of the band of highly excited Rydberg states, though the formal solution for longer pulses poses no problems within our procedure. With this solution quantitative results are presented for ionization of the model hydrogen atom from different l states but of the same $n=4$ by a linearly polarized 100-fs pulse of the frequency resonant to the $n=4\rightarrow n=40$ transition. The initial states are intentionally chosen in such a way that either nonresonant or resonant migration of population to higher-l Rydberg states takes place. From the results obtained, we draw conclusions about the initial-state lifetime, redistribution of population versus laser intensity, efficiency of migration to higher-l Rydberg states, threshold laser intensities stabilizing the model atom against ionization, and the stabilizing mechanisms versus the initial-state choice.

Our paper is organized as follows. Section II is devoted to presentation of a formal theory. In Sec. II A we introduce the model of ionization via high-Rydberg states, in which only nonresonant migration of population to higher-l Rydberg states via degenerate Raman coupling takes place. It is also shown in this section how to calculate (analytically, in principle) the Raman coupling parameters. In Sec. II B this model is solved in terms of continued fractions and the relation to the above-threshold-ionization problem of Deng and Eberly [12] is pointed out. Section II C concerns the model in which the population from the directly excited Rydberg states of a fixed l migrates to Rydberg states of l increased by 2 through a state degenerate with the initial state of the process. In Sec. III the analytical solutions are applied to different initial states in the model hydrogen atom and comparative studies are performed with emphasis on stabilization. We end the paper by presenting in Sec. IV the main conclusions derived from our model studies.

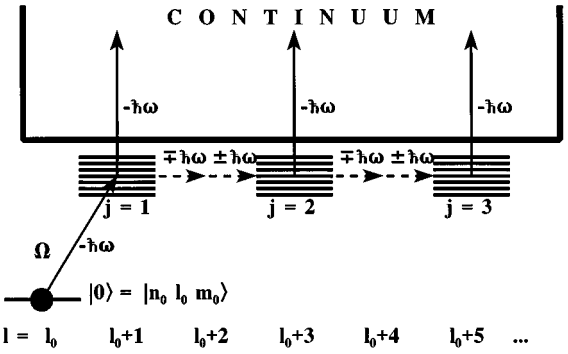

FIG. 1. The model of ionization from a low-lying atomic state $|0\rangle=1n_0l_0m_0\rangle$ via a band of high-lying Rydberg states ($n\gg1$), with the inclusion of nonresonance migration of population to higher-angular-momentum Rydberg states due to degenerate Raman transitions (dashed arrows). The sign at the photon energy corresponds to either absorption ($-$) or emission ($+$) of a photon. By $j=1,2,\ldots,N$ we label Rydberg quasicontinua of angular-momentum quantum number $l=l_0+(2j-1)$.

II. THEORY

A. The model with nonresonance migration and coupling parameters

Figure 1 shows the basic model of nominal two-photon ionization of the hydrogen atom from an initial state $|0\rangle=|n_0l_0m_0\rangle$ via a band of high-lying Rydberg states of $n\gg1$. The principal quantum number n_0 of the initial state is assumed to be low enough for this state to satisfy the condition of being well isolated from all other lower- and higher-lying states. The choice of this initial state is made so that after absorption of one electric-dipole photon only those higher-lying Rydberg states could be excited whose angular-momentum quantum number l is increased by one with respect to l_0 of the initial state. An exemplifying initial state ensuring this condition (but not the only one) is the so-called circular state $|0\rangle=|n_0l_0=m_0=n_0-1\rangle$ exposed to light linearly polarized along the z axis. Photons of such light leave the magnetic quantum number m_0 of the atomic state unchanged, thus closing the $l_0\rightarrow l_0-1$ excitation channel. In our model, photons are provided by a rectangular optical pulse turned on at $t=0$. This pulse interacts with the atom through the Hamiltonian taken in the momentum form, $V=(-e/m_ec)\vec{A}\cdot\vec{p}$, where the vector potential is spatially independent. The term with A^2 was rejected in the above interaction Hamiltonian as it shifts all states equally by the ponderomotive energy, $e^2A_0^2/4m_ec^2$. By absorbing one photon, the atom from its initial state $|0\rangle=|n_0l_0m_0\rangle$ is excited to a band of Rydberg states with the momentum $l=l_0+1$, lying slightly below the ionization threshold. These Rydberg states with $n\gg1$ form what will be referred to as the first Rydberg quasicontinuum. This quasicontinuum will be labeled by $j=1$. By $V_{0,n1}$ we denote the matrix element for the coupling between the initial state and an n state in the $j=1$ quasicontinuum. The essential point of the model is that the population which reached the $j=1$ quasicontinuum ($l_1=l_0+1$) is allowed to migrate to higher-angular-momentum Rydberg quasicontinuum, namely, to the $j=2$ quasicontinuum ($l_2=l_0+3$), then to the $j=3$ quasicontinuum ($l_3=l_0+5$), and so on $[l_j=l_0+(2j-1)]$, due to degenerate Raman transitions involving both discrete and continuum states of the appropriate angular momenta as intermediaries. These degenerate Raman transitions are schematically shown by dashed arrows in Fig. 1. In the basic model, no resonant intermediate state is assumed to be involved in the Raman coupling between Rydberg states from the neighboring quasicontinua. Specifically, this assumption is satisfied always if the initial state is a circular state $|0\rangle=|n_0l_0=m_0=n_0-1\rangle$ (but not only in this case). A generalization of the basic model to include an intermediate resonance in the Raman coupling between the first ($j=1$) and second ($j=2$) quasicontinua will be considered later on.

We shall describe the nonresonant Raman coupling between any two high-lying Rydberg states by $D_{ba}=(i/\hbar)M_{ba}$, where M_{ba} is the standard Raman matrix element provided by the second-order perturbation theory. Each high-lying Rydberg state is specified by $n\gg n_0$, $l=l_0+(2j-1)$, and $m=m_0$, under our assumptions concerning the choice of the initial state and the light polarization (linear along the z axis). Specifically, in the application of our model we will concentrate later on $n_0=4$ and $n\simeq40$ corresponding to the exciting-photon energy $\hbar\omega\simeq\mathcal{R}/16\simeq0.85$eV where $\mathcal{R}$ is the Rydberg constant. The two high-lying Rydberg states ($n\simeq40$) which are Raman coupled can belong either to the same quasicontinuum of a given l or to two neighboring quasicontinua differing by two in l, but both states undergo one-photon ionization, with continuum-continuum transitions ignored in our model. As a result, the second-order matrix element M_{ba} acquires an imaginary part and D_{ba} is generally expressible as [11]

$$D_{ba}=(1+iq_{ba})\sqrt{\gamma_b\gamma_a}/2, \tag{1}$$

where $\gamma_{b(a)}$ stands for Fermi's golden rule ionization rate of $|b\rangle(|a\rangle)$ to the continuum that is common for these two Rydberg states. If $|b\rangle$ and $|a\rangle$ belong to two neighboring quasicontinua, there exist intermediate continuous states of only one angular momentum. However, for $|b\rangle$ and $|a\rangle$ from the same quasicontinuum, intermediate continuous states of two different angular momenta are accessible and then $\gamma_{b(a)}$ must be understood as a sum over partial ionization rates. By q_{ba} we denoted the Fano-like parameter defined as

$$q_{ba}=\frac{(1/\hbar)\sum_{\pm,i\neq r}[(V_{bi}V_{ia}/(E_a-E_i\pm\hbar\omega)]}{\sqrt{\gamma_b\gamma_a}/2}, \tag{2}$$

where the sum is extended over rotating-wave and counter-rotating-wave terms, as well as over all bound and free atomic states with the preclusion of the resonant ones.

The above-mentioned summation over intermediate states can be performed exactly by the use of the Coulomb Green's function [6]. In this paper, we prefer, however, an approximate approach based on the fact that the energy of the photon involved (~0.85eV) is much higher than the energy difference between high-lying and even moderately high-lying Rydberg states. Exploiting this fact, we formally split the space of intermediate states into two groups, namely, the discrete states with their principal quantum number $n\leqslant\overline{n}$ and the rest of the states. For a fixed photon energy $\hbar\omega$, $\overline{n}$ is chosen to be large enough for the relation $|E_a-E_n|\ll\hbar\omega$ to

be well fulfilled. Up to $n=\overline{n}$ we explicitly compute the sum in the numerator of Eq. (2), but for $n>\overline{n}$ we expand the summand in the inverse powers of $\hbar\omega$ and retain only the leading term. The last step in this procedure is what is usually referred to as the high-frequency approximation. An essential part of the leading term turns out to be reduced to a simple form and we shall show it now. According to the procedure described above, we first replace the two-photon matrix element from the numerator of Eq. (2) by its approximate form:

$$\sum_{\pm,i\neq r}\frac{V_{bi}V_{ia}}{E_a-E_i\pm\hbar\omega}\simeq\left(\frac{eA_0}{2m_ec}\right)^2\frac{2}{\hbar}\left[\sum_{\substack{i\leqslant n\\ \neq r}}(p_z)_{bi}(p_z)_{ia}\frac{\omega_{ai}}{\omega_{ai}^2-\omega^2}+\frac{1}{\omega^2}\right.$$
$$\left.\times\left(\sum_i(p_z)_{bi}(p_z)_{ia}\omega_{ia}-\sum_{\substack{i\leqslant n\\ \neq r}}(p_z)_{bi}(p_z)_{ia}\omega_{ia}-\sum_r(p_z)_{br}(p_z)_{ra}\omega_{ra}\right)\right], \tag{3}$$

where $\omega_{\beta\alpha}=(E_\beta-E_\alpha)/\hbar$. Then, we use the relation $(p_z)_{ia}\omega_{ia}=-i(\dot{p}_z)_{ia}=i(\partial V/\partial z)_{ia}$, valid for an atomic potential V, to find that

$$\sum_i(p_z)_{bi}(p_z)_{ia}\omega_{ia}=-\hbar\left(\frac{\partial V}{\partial z}\frac{\partial}{\partial z}\right)^*_{ab}. \tag{4}$$

For the hydrogenic potential, $V=-e^2/r$, the resulting single matrix element is calculated straightforwardly by applying standard techniques of angular-momentum algebra. For the states specified as $|a\rangle=|nlm\rangle$ and $|b\rangle=|n'l'm'=m\rangle$, one obtains in this way the off-diagonal sum rule

$$\sum_i(p_z)_{bi}(p_z)_{ia}\omega_{ia}=-\hbar e^2\left[(\alpha_0\delta_{l',l}+\alpha_+\delta_{l',l+2}\right.$$
$$+\alpha_-\delta_{l',l-2})\left(\frac{1}{r^2}\frac{d}{dr}\right)_{nl,n'l'}$$
$$+[\beta_0\delta_{l',l}+(l+3)\alpha_+\delta_{l',l+2}$$
$$\left.-(l-2)\alpha_-\delta_{l',l-2}]\left(\frac{1}{r^3}\right)_{nl,n'l'}\right], \tag{5}$$

where $[f(r)]_{nl,n'l'}=\int_0^\infty R^*_{nl}(r)f(r)R_{n'l'}(r)r^2dr$ is a purely radial matrix element, δ_{pq} is the Kronecker symbol reflecting the selection rules for two-photon electric-dipole transitions, and the rest are the angular-momentum-algebra coefficients of the form

$$\alpha_0=\frac{2l(l+1)-1-2m^2}{(2l-1)(2l+3)}, \tag{6}$$

$$\alpha_+=\frac{1}{2l+3}\left(\frac{[(l+1)^2-m^2][(l+2)^2-m^2]}{(2l+1)(2l+5)}\right)^{1/2}, \tag{7}$$

$$\alpha_-=\frac{1}{2l-1}\left(\frac{(l^2-m^2)[(l-1)^2-m^2]}{(2l+1)(2l-3)}\right)^{1/2}, \tag{8}$$

$$\beta_0=\frac{l(l+1)-3m^2}{(2l-1)(2l+3)}. \tag{9}$$

Thanks to the summation rule established and using the relation $(p_z)_{\beta\alpha}=im_e\omega_{\beta\alpha}z_{\beta\alpha}$, we finally express the required matrix element from Eq. (2) as

$$\sum_{\pm,i\neq r}\frac{V_{bi}V_{ia}}{E_a-E_i\pm\hbar\omega}$$
$$\simeq-2a_0^3\left(\frac{2\mathcal{R}}{\hbar\omega}\right)^2\frac{e^2A_0^2}{4m_ec^2}$$
$$\times\left[(\alpha_0\delta_{l,l'}+\alpha_+\delta_{l',l+2}+\alpha_-\delta_{l',l-2})\left(\frac{1}{r^2}\frac{d}{dr}\right)_{nl,n'l'}\right.$$
$$+[\beta_0\delta_{l',l}+(l+3)\alpha_+\delta_{l',l+2}-(l-2)\alpha_-\delta_{l',l-2}]$$
$$\times\left(\frac{1}{r^3}\right)_{nl,n'l'}-\frac{m_e^2}{\hbar e^2}\left(\sum_r\omega_{br}\omega_{ra}^2z_{br}z_{ra}\right.$$
$$\left.\left.+\sum_{\substack{i\leqslant n\\ \neq r}}\frac{\omega_{bi}\omega_{ia}^4}{\omega_{ia}^2-\omega^2}z_{bi}z_{ia}\right)\right], \tag{10}$$

where a_0 and $2\mathcal{R}$ are the atomic units of length and energy, respectively, while $e^2A_0^2/(4m_ec^2)$ is the quiver (ponderomotive) energy of the free electron in an electromagnetic field.

Equation (10) is convenient for two reasons. First, the incorporated radial matrix elements can be found analytically for hydrogen and, secondly, the value of the sum over $i\leqslant\overline{n}$ is not too sensitive to the choice of $\overline{n}$ and for optical photons a rather low $\overline{n}$ ensures correct estimation of the sum. Moreover, Eq. (10) has correct marginal behavior for $|b\rangle=|a\rangle=|nlm\rangle$. In that diagonal case, the first two terms in the large square brackets take a particularly simple form because then

$$\left(\frac{1}{r^2}\frac{d}{dr}\right)_{nl,nl}=-\frac{1}{2}R_{nl}^2(0)=-2/(n^3a_0^3)\delta_{l0}$$

and

$$(r^{-3})_{nl,nl}=2/[l(l+1)(2l+1)n^3a_0^3]$$

With only these two terms retained, Eq. (10) reduces to

$$\sum_{\pm,i\neq r}\frac{|V_{ai}|^2}{E_a-E_i\pm\hbar\omega}\simeq\frac{e^2A_0^2}{4m_ec^2}\left(\frac{2\mathcal{R}}{\hbar\omega}\right)^2\frac{4}{3n^3}\times\left(\delta_{l0}+3\frac{3m^2-l(l+1)}{l(l+1)(2l-1)(2l+1)(2l+3)}\right),\qquad(11)$$

which is the 30-year-old result of Ritus [13,14] (in fact, diminished by the ponderomotive energy due to our neglect of the A^2 term in the interaction Hamiltonian).

We will use Eq. (10) when calculating the two-photon matrix elements inherent in q_{ba} [Eq. (2)], and apply the recent prescription of Feldman, Fulton, and Judd [15] when finding the needed ionization rates from high-Rydberg states. In this way, we will complete all Raman couplings D_{ba} of our model. These Raman couplings play the role of linking parameters in the appropriate equations of motion for the Schrödinger population amplitudes of high-Rydberg states. Let b_0 stand for the Schrödinger amplitude of the initial state, and b_{nj} for the Schrödinger amplitude of an n state in the j quasicontinuum. We write the evolution equations for the amplitudes in the rectangular-pulse and rotating-wave approximations and then apply to them the Laplace transformation ($t\rightarrow s$, $b_0\rightarrow\tilde{b}_0$ and $b_{nj}\rightarrow\tilde{b}_{nj}$). It leads to an infinite set of coupled algebraic equations. The appropriate Laplace equation for the initial state is obtained along this line as

$$s\tilde{b}_0=1-\frac{i}{\hbar}\sum_n V_{0,n1}\tilde{b}_{n1},\qquad(12)$$

whereas the equation for the first quasicontinuum ($j=1$) looks like

$$(s-i\delta_{n1})\tilde{b}_{n1}=-\frac{i}{\hbar}V_{n1,0}\tilde{b}_0-\sum_{n'}D_{n1,n'1}\tilde{b}_{n'1}-\sum_{n'}D_{n1,n'2}\tilde{b}_{n'2},\qquad(13)$$

while for the next quasicontinua ($j\geqslant 2$) we have

$$(s-i\delta_{nj})\tilde{b}_{nj}=-\sum_{n'}D_{nj,n'j}\tilde{b}_{n'j}-\sum_{n'}D_{nj,n'j-1}\tilde{b}_{n'j-1}-\sum_{n'}D_{nj,n'j+1}\tilde{b}_{n'j+1},\qquad(14)$$

where δ_{nj} is the field-free detuning from one-photon ($j=1$) or Raman multiphoton ($j\geqslant 2$) resonance, and $D_{nj,n'j'}$ should be understood as the Raman coupling between the n state in the j quasicontinuum and the n' state in the j' quasicontinuum. We remind the reader that the angular momentum of states in a given quasicontinuum is determined by $l_j=l_0+(2j-1)$, and all these states are labeled by the same magnetic number as the initial state because of the assumed linear polarization of light along the z axis.

B. Approximate solution of the model with nonresonance migration

It is impossible to find an exact analytical solution in a compact form to the set of Eqs. (12)–(14) if the laser pulse is short and of high intensity, because an extremely high number of Rydberg states is generally excited due to both large laser bandwidth and ionization broadening of the states. It is thus unavoidable to simplify appropriately the set of Eqs. (12)–(14) if one wants to treat the process within an analytical procedure. The main problem in finding a compact analytical solution to the set of interest is the actual n dependence of the included Raman couplings. We have investigated this dependence. Precisely, exploiting Eq. (10), we calculated these couplings for a band of Rydberg states around $n=40$, assuming photon energy resonant with the $n_0=4\rightarrow n=40$ transition. For the Raman couplings between Rydberg states within the same quasicontinuum ($|a\rangle=|nl_jm_0\rangle$, $|b\rangle=|n'l_jm_0\rangle$), we found that D_{ba} changed a little only when n and n' were varied around 40, and it did not differ significantly from D_{aa}, i.e., when $n=n'$. Such behavior encouraged us to replace all Raman couplings within a given quasicontinuum by a single coupling representative for this quasicontinuum, precisely, $D_{nj,n'j}$ by D_{jj}. In the case of the coupling between the states from the neighboring quasicontinua ($|a\rangle=|nl_jm_0\rangle$, $|b\rangle=|n'l_{j'},m_0\rangle$), we distinguish between the cases of $n=n'$ and $n\neq n'$. In the first case, D_{ba} is small as the summation rule of Eq. (5) gives zero. In the second case, D_{ba} behaves similarly to the couplings between states within the same quasicontinuum. On this basis we neglect the interquasicontinuum coupling between states of the same n, and replace all other couplings between two neighboring quasicontinua by a single coupling representative for a given pair of quasicontinua, namely, $D_{nj,n'j'}$ by $D_{jj'}$. Briefly, both the intraquasicontinuum and interquasicontinuum couplings are approximated to be n independent but they are still left to be l dependent. As the representative couplings we choose those between the Rydberg states with the principal quantum numbers equal to 40 and 41. As a matter of fact, the above approximation of Raman couplings is justified if only those Rydberg states are populated whose principal quantum number do not depart markedly from $n=40$. In practice, it is the case of not too short and not too intense laser pulse. If a laser pulse does not fulfill these limitations, states with principal quantum numbers differing significantly from $n=40$ will be populated as well. The appropriate Raman couplings between these additional states will, even considerably, differ from the chosen representative couplings due to the rough $1/(nn')^{3/2}$ dependence. However, we will apply the approximation of the representative couplings also in this case, being aware that the atom we deal with ceases to be a real hydrogen atom and becomes a model one. To assess how far the behavior of this model atom departs from that of the real hydrogen atom, in a short highly intense-laser pulse, numerical simulations are necessary.

According to the above approximation of the Raman coupling parameters, we simplify Eqs. (12)–(14) to the following set:

$$s\tilde{b}_0 = 1 - i\Omega K_1, \tag{15}$$

$$(s - i\delta_{n1})\tilde{b}_{n1} = -i\Omega\tilde{b}_0 - D_{11}K_1 - D_{12}K_2, \tag{16}$$

$$(s - i\delta_{nj})\tilde{b}_{nj\geq 2} = -D_{jj}K_j - D_{jj-1}K_{j-1} - D_{jj+1}K_{j+1}, \tag{17}$$

where

$$K_j = \sum_n \tilde{b}_{nj}, \tag{18}$$

and Ω is the representative Rabi frequency for the transition from the initial state to the first quasicontinuum. The essential point is that the set of approximate Eqs. (15)–(17) is structurally similar to the set obtained by Deng and Eberly [12] for their model of a different phenomenon, namely, above-threshold ionization (ATI) with infinite sequence of continua. Formally, their equations can be obtained from ours by neglecting the diagonal Raman couplings ($D_{jj}=0$), and replacing the remaining off-diagonal Raman couplings $D_{jj'}$, by usual one-photon free-free couplings, precisely, $D_{jj\pm 1}$ by $iV_{jj\pm 1}$. Recognizing the above-stated structural similarity, we adopt the solution procedure of Deng and Eberly to the problem of our interest. Following their line, we divide Eq. (16) by $s - i\delta_{n1}$ and Eq. (17) by $s - i\delta_{nj}$ and then sum the results over all Rydberg states. Equations (16) and (17) are then transformed into

$$(1 + P_1 D_{11})K_1 = -i\Omega P_1\tilde{b}_0 - P_1 D_{12}K_2, \tag{19}$$

$$(1 + P_j D_{jj})K_{j\geq 2} = -P_j D_{jj-1}K_{j-1} - P_j D_{jj+1}K_{j+1}, \tag{20}$$

where

$$P_j = \sum_n \frac{1}{s - i\delta_{nj}}. \tag{21}$$

We solve Eq. (20) by the method of subsequent eliminations, first eliminating the last Rydberg quasicontinuum with $j=N$. For $j=N$, the second right-hand side term in Eq. (20) vanishes and we can express K_N by K_{N-1}. Having expressed K_N by K_{N-1}, we then express K_{N-1} by K_{N-2}, and so on. In this way one finds from Eq. (20) the recursion relation

$$K_{j\geq 2} = -P_j G_j D_{jj-1}K_{j-1}, \tag{22}$$

with G_j having the form of a continued fraction. For all j (also $j=1$), G_j can be expressed by the recurrence formula

$$G_j = \frac{1}{1 + P_j D_{jj}(1 - (D_{jj+1}^2/D_{jj})P_{j+1}G_{j+1})}, \tag{23}$$

fulfilling the boundary condition

$$G_N = \frac{1}{1 + P_N D_{NN}}. \tag{24}$$

Starting with this condition, we create step by step G_{N-1} from G_N, G_{N-2} from G_{N-1}, . . . , and finally G_1 from G_2. By the use of Eq. (22), we then express K_2 by K_1 and substitute this K_2 into Eq. (19). After this substitution, Eqs. (19) and (15) form a set with respect to $\tilde{b}_0$ and K_1. When solved, this set gives

$$\tilde{b}_0 = \frac{1}{s + \Omega^2 P_1 G_1}, \tag{25}$$

$$K_1 = -i\Omega P_1 G_1\tilde{b}_0. \tag{26}$$

Applying this solution, we find from Eqs. (16) and (17) that for all $j=1,2,\ldots,N$,

$$\tilde{b}_{nj} = \frac{1}{s - i\delta_{nj}}\frac{K_j}{P_j}, \tag{27}$$

where, in conformity with Eqs. (22) and (26),

$$K_{j\geq 2} = (-1)^j i\Omega\left(\prod_{k=1}^{j-1} D_{k\,k+1}\right)\left(\prod_{k=1}^{j} P_k G_k\right)\tilde{b}_0. \tag{28}$$

Formally, Eq. (28) can be extended to include the case of $j=1$ as well, if we assume that $\Pi_{k=1}^0$ is equal to 1. Equations (25) and (27), along with Eqs. (28), (23), and (21), constitute the solution of our model in the Laplace domain.

Analytical transformation of the above Laplace solution to the time domain needs additional approximations. Following the papers [9,16] on the related subjects, we approximate the Rydberg energy structure for $n \gg 1$ by an equidistant structure. The limitations of this harmonic approximation are as those of the previous approximation of representative Raman couplings. We simply write $\delta_{nj} = \delta_j + \nu\Delta_j$, with δ_j being the detuning from the Rydberg state closest to resonance in the j quasicontinuum, Δ_j the appropriate spacing, and $\nu = 0, \pm 1, \pm 2, \ldots$ the index numbering the states up and down from the resonant one ($\nu = 0$). Then, we set $\Delta_j = \Delta$ and $\delta_j = \delta = 0$ for all $j = 1,2,\ldots,N$ because of the actual orbital degeneracy in hydrogen and the assumed resonance between the initial state $|0\rangle$ and the Rydberg state of $n=40$ to which $\nu = 0$ is ascribed. These assumptions allow us to apply the standard coth representation for P_j [17], namely, $P_j = P = (\pi/\Delta)(1+\mu)/(1-\mu)$, where $\mu = \exp(-Ts)$, with $T = 2\pi/\Delta$ having the sense of the classical Kepler period of the resonant state of $n=40$ ($\Delta = 6.46\times 10^{11}$ s$^{-1} \rightarrow T = 9.7$ ps). With this P, we follow the prescription of Stey and Gibberd [17], i.e., we expand both $\tilde{b}_0$ and $\tilde{b}_{nj}$ in a power series of μ and then transform each term of this expansion. The first term (with μ^0) is known to contribute to all times, the second term (with μ^1) to times longer than the Kepler period, the third term (with μ^2) to times longer than twice the Kepler period, and so on. We assume the laser pulse duration to be shorter than the Kepler period, and thus retain only the first term in this expansion. The transformation of this term to the time domain is straightforward and results in the following Schrödinger amplitudes:

$$b_0 = e^{-2\pi\rho\tau}, \tag{29}$$

$$b_{\nu j}=g_\nu(\tau)e^{i2\pi\nu\tau}A_j\prod_{k=1}^{j}G_K(0), \tag{30}$$

where $\tau=t/T\leqslant 1$ is the pulse duration in units of the Kepler period, $G_K(0)$ is the value of the continued fraction G_K at $\mu=0$, and

$$A_j=i2(-\pi)^j\sqrt{u}\prod_{k=1}^{j-1}(D_{k\,k+1}/\Delta)\quad(A_1=-i2\pi\sqrt{u}), \tag{31}$$

$$g_\nu(\tau)=\frac{1-e^{-2\pi(\rho+i\nu)\tau}}{2\pi(\rho+i\nu)}, \tag{32}$$

$$\rho=\pi u G_1(0),\quad u=(\Omega/\Delta)^2. \tag{33}$$

Thus, after a short optical pulse of $\tau>1$, the population that has been left in the initial state of the process is $|b_0|^2=\exp[-4\pi\tau\mathrm{Re}(\rho)]$, while the population transferred to the j quasicontinuum, obtained by integrating $|b_{\nu j}|^2$ over ν, amounts to

$$W_j\overset{\tau\leqslant 1}{=}\left|A_j\prod_{k=1}^{j}G_k(0)\right|^2\frac{1-e^{-4\pi\tau\mathrm{Re}(\rho)}}{4\pi\mathrm{Re}(\rho)}. \tag{34}$$

These simple formulas deserve four comments. First, the exponential decay law of the initial state holds only in the short-pulse scale of $\tau\leqslant 1$. It breaks for longer pulses of $\tau>1$ due to the higher-order terms which would have to be included in the Stey-Gibberd expansion of the Laplace solution. Secondly, the decay rate of the initial state in the short-pulse scale amounts to

$$R_0=2\Delta\mathrm{Re}(\rho)=2\pi u\Delta\mathrm{Re}[G_1(0)]$$
$$=\frac{2\pi}{\hbar}|V_{0,1}|^2(\hbar\Delta)^{-1}\mathrm{Re}[G_1(0)] \tag{35}$$

and, after recognizing $(\hbar\Delta)^{-1}$ as the density of states, it can be interpreted as Fermi's golden rule excitation rate of the first quasicontinuum modified by $\mathrm{Re}[G_1(0)]$, i.e., the effect of nonresonant Raman couplings in the model. This modification is, obviously, intensity dependent. Thirdly, there is evident formal resemblance of the final short-pulse formulas of our model to the corresponding formulas of Deng and Eberly [12] for their model of ATI with a sequence of continua. This formal resemblance becomes obvious if one realizes that our first Rydberg quasicontinuum, of the actual discrete structure not resolved by a short pulse, is a counterpart of the first ATI continuum, and our higher-angular-momentum quasicontinua are counterparts of the subsequent ATI continua. Needless to say, in this context bound-bound Raman couplings of our model obviously differ from one-photon free-free couplings of the ATI model. Finally, due to the approximations of representative Raman couplings and equal spacing of high-Rydberg states, Eqs. (29)–(34) can be considered as only a rough analytical description of the population redistribution in a real hydrogen atom by a short, intense-laser pulse.

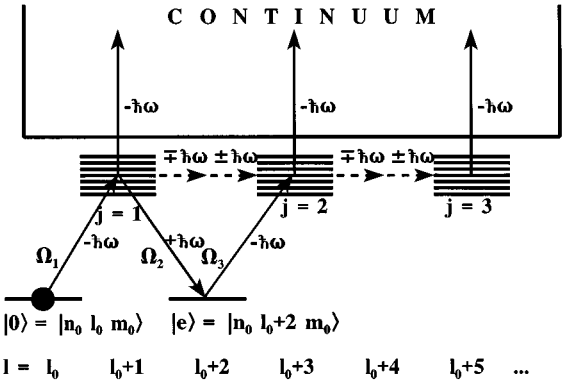

FIG. 2. The model of ionization from a low-lying atomic state $|0\rangle=|n_0l_0m_0\rangle$ via a band of high-lying Rydberg states ($n\gg 1$), in which resonance migration of population from the first to second Rydberg quasicontinua takes place due to the existence of the state $|e\rangle$ of angular momentum l_0+2 degenerate with the initial state $|0\rangle=|n_0l_0m_0\rangle$.

C. The model with resonance migration and its solution

Retaining the approximations introduced in the preceding section, we now generalize the model to include the case when the Rydberg states from the first quasicontinuum can be resonantly coupled to a state $|e\rangle$ degenerate with the initial state $|0\rangle$ (see Fig. 2). For example, this is the case of the $|0\rangle=4s$ initial state. In this case, the degenerate companion $|e\rangle=4d$ opens the resonance channel of migration $np\rightarrow 4d\rightarrow nf$ from the first to second Rydberg quasicontinua.

According to Fig. 2, we denote by Ω_1 the representative Rabi frequency for the transition between the initial $|0\rangle$ state and the first Rydberg quasicontinuum, and by $\Omega_{2(3)}$ the appropriate representative Rabi frequencies for the transition between the resonant $|e\rangle$ state and the first (second) quasicontinua. The resonant $|e\rangle$ state must be treated now on the same footing as the initial $|0\rangle$ state and, as a result, instead of the previous Eqs. (15)–(17) we have the generalized set

$$s\tilde{b}_0=1-i\Omega_1K_1, \tag{36}$$

$$s\tilde{b}_e=-i\Omega_2K_1-i\Omega_3K_2, \tag{37}$$

$$(s-i\delta_{n1})\tilde{b}_{n1}=-i\Omega_1\tilde{b}_0-i\Omega_2\tilde{b}_e-D_{11}K_1-D_{12}K_2, \tag{38}$$

$$(s-i\delta_{n2})\tilde{b}_{n2}=-i\Omega_3\tilde{b}_e-D_{22}K_2-D_{21}K_1-D_{23}K_3, \tag{39}$$

$$(s-i\delta_{nj})\tilde{b}_{nj\geqslant 3}=-D_{jj}K_j-D_{jj-1}K_{j-1}-D_{jj+1}K_{j+1}. \tag{40}$$

This new set can be solved along the line similar to that we applied previously in Sec. II B. Briefly, we first divide Eqs. (38)–(40) by $s-i\delta_{nj}$ and then sum the resulting equations over all n. In this way, one obtains from Eqs. (36)–(40) a set for the variables $\tilde{b}_0,\tilde{b}_e,K_1,K_2$, and $K_{j\geqslant 3}$. Because the obtained equation for $K_{j\geqslant 3}$ is of the same structure as Eq. (20), its solution is still given by Eq. (22) with the only change that now $j\geqslant 3$. Applying this solution, we find by subsequent eliminations that

$$\tilde{b}_0=\frac{1}{C}[s+P_1G_1(\Omega_2-D_{12}P_2G_2\Omega_3)^2+P_2G_2\Omega_3^2], \tag{41}$$

$$\tilde{b}_e=-\frac{1}{C}P_1G_1\Omega_1(\Omega_2-D_{12}P_2G_2\Omega_3), \tag{42}$$

$$K_1=-\frac{i}{C}P_1G_1\Omega_1(s+P_2G_2\Omega_3^2), \tag{43}$$

$$K_{j\geqslant 2}=\frac{i}{C}(-1)^j\Omega_1[s+(\Omega_2\Omega_3/D_{12})]\times\left(\prod_{k=1}^{j-1}D_{k\,k+1}\right)\left(\prod_{k=1}^{j}P_kG_k\right), \tag{44}$$

where

$$C=(s+P_1G_1\Omega_1^2)(s+P_2G_2\Omega_3^2)+P_1G_1(\Omega_2-D_{12}P_2G_2\Omega_3)^2s. \tag{45}$$

With this result, we obtain from Eqs. (38)–(40) the following Laplace solution for Rydberg states:

$$\tilde{b}_{nj}=\frac{1}{s-i\delta_{nj}}\frac{K_j}{P_j}. \tag{46}$$

When transforming the above Laplace solutions to the time domain, we again focus on the short-pulse case only ($\tau\leqslant 1, P_j\rightarrow\pi/\Delta_j=\pi/\Delta$) and assume exact $|0\rangle\rightarrow n=40$ resonance. In this case, our C [Eq. (45)] becomes a quadratic equation with respect to the Laplace variable s. As a result, the time originals are found straightforwardly in the form

$$b_0\overset{\tau\leqslant 1}{=}\frac{1}{x_+-x_-}[[x_++\alpha-\pi G_1(0)u_1]e^{2\pi x_+\tau}-[x_-+\alpha-\pi G_1(0)u_1]e^{2\pi x_-\tau}], \tag{47}$$

$$b_e\overset{\tau\leqslant 1}{=}-\pi G_1(0)\sqrt{u_1}\left(\sqrt{u_2}-\pi G_2(0)\sqrt{u_3}\frac{D_{12}}{\Delta}\right)\times\frac{e^{2\pi x_+\tau}-e^{2\pi x_-\tau}}{x_+-x_-}, \tag{48}$$

$$b_{\nu 1}\overset{\tau\leqslant 1}{=}-e^{-i2\pi\nu\tau}\frac{G_1(0)\sqrt{u_1}}{x_+-x_-}\times[[x_++\pi G_2(0)u_3]g(\nu-ix_+,\tau)-[x_-+\pi G_2(0)u_3]g(\nu-ix_-,\tau)], \tag{49}$$

$$b_{\nu j\geqslant 2}\overset{\tau\leqslant 1}{=}-ie^{-i2\pi\nu\tau}\frac{A_j}{2\pi(x_+-x_-)}\left(\prod_{k=1}^{j}G_k(0)\right)\times\left[\left(x_++\frac{\sqrt{u_2u_3}}{D_{12}/\Delta}\right)g(\nu-ix_+,\tau)-\left(x_-+\frac{\sqrt{u_2u_3}}{D_{12}/\Delta}\right)g(\nu-ix_-,\tau)\right], \tag{50}$$

where $u_k=(\Omega_k/\Delta)^2$ for $k=1,2$, and 3, A_j is defined by Eq. (31) with the change $u\rightarrow u_1$,

$$g(\nu-ix_\pm,\tau)=\frac{e^{i2\pi\tau(\nu-ix_\pm)}-1}{\nu-ix_\pm}, \tag{51}$$

and $x_\pm$ are the roots of the quadratic equation $x^2+\alpha x+\beta=0$ with the coefficients

$$\alpha=\pi G_1(0)\left[u_1+\left(\sqrt{u_2}-\pi G_2(0)\sqrt{u_3}\frac{D_{12}}{\Delta}\right)^2\right]+\pi G_2(0)u_3, \tag{52}$$

$$\beta=\pi^2G_1(0)G_2(0)u_1u_3. \tag{53}$$

Integrating the squared modulus of the amplitudes $b_{\nu j}$ over ν, we arrive at the following total populations transferred to the subsequent Rydberg quasicontinua:

$$W_1\overset{\tau\leqslant 1}{=}\pi u_1\left|\frac{G_1(0)}{x_+-x_-}\right|^2\times\left\{|x_++\pi G_2(0)u_3|^2\frac{e^{4\pi\tau\mathrm{Re}(x_+)}-1}{\mathrm{Re}(x_+)}+|x_-+\pi G_2(0)u_3|^2\frac{e^{4\pi\tau\mathrm{Re}(x_-)}-1}{\mathrm{Re}(x_-)}-4\mathrm{Re}\left[[x_++\pi G_2(0)u_3][x_-+\pi G_2(0)u_3]^*\times\frac{e^{2\pi\tau(x_++x_-^*)}-1}{x_++x_-^*}\right]\right\}, \tag{54}$$

$$W_{j\geqslant 2}\overset{\tau\leqslant 1}{=}\frac{1}{4\pi|x_++x_-|^2}\left|A_j\prod_{k=1}^{j}G_k(0)\right|^2\times\left\{\left|x_++\frac{\sqrt{u_2u_3}}{D_{12}/\Delta}\right|^2\frac{e^{4\pi\tau\mathrm{Re}(x_+)}-1}{\mathrm{Re}(x_+)}+\left|x_-+\frac{\sqrt{u_2u_3}}{D_{12}/\Delta}\right|^2\frac{e^{4\pi\tau\mathrm{Re}(x_-)}-1}{\mathrm{Re}(x_-)}-4\mathrm{Re}\left[\left(x_++\frac{\sqrt{u_2u_3}}{D_{12}/\Delta}\right)\left(x_-+\frac{\sqrt{u_2u_3}}{D_{12}/\Delta}\right)^*\times\frac{e^{2\pi\tau(x_++x_-^*)}-1}{x_++x_-^*}\right]\right\}. \tag{55}$$

One evident effect of the resonant state $|e\rangle$ between the first and second quasicontinua is that no simple exponential decay law of the initial state $|0\rangle$, with the rate R_0 given by Eq. (35), is valid any longer. Other effects of $|e\rangle$ on the redistribution of population are the subject discussed in Sec. III.

III. RESULTS

Now we apply the theory developed in Sec. II to the ionization processes starting from different initial states. The initial states under further considerations are chosen to share

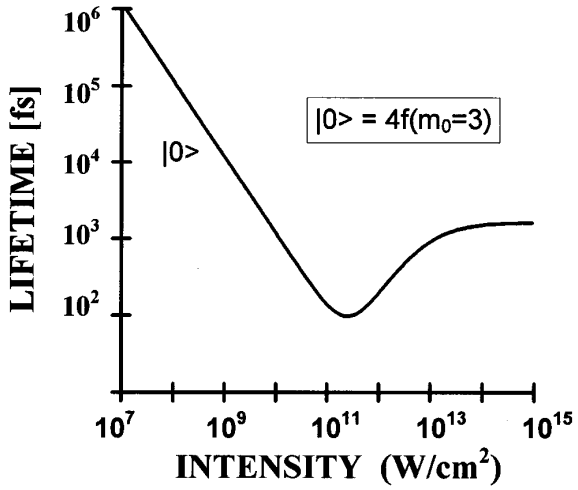

FIG. 3. Lifetime, $1/R_0$, of the circular $4f(m_0=3)$ initial state versus laser intensity. The light beam is assumed to be linearly polarized of a frequency resonant to the $n_0=4\rightarrow n=40$ transition in hydrogen.

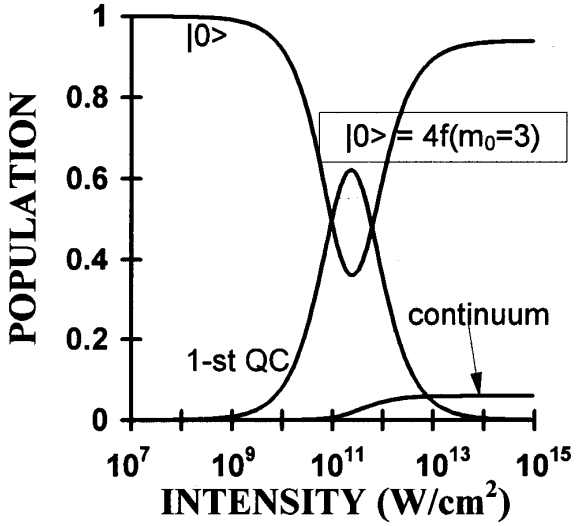

FIG. 4. The population of the initial state $|0\rangle=4f(m_0=3)$, the first Rydberg quasicontinuum (QC) of $l=4$, and the continuum versus laser intensity, for a 100-fs laser pulse. The polarization and frequency of light are as in Fig. 3.

the same principal quantum number $n_0=4$ but to differ with respect to the angular-momentum quantum number l_0. One group of the initial states is formed by the circular $4f(m_0=3)$ state and the $4d(m_0=2)$ state. The initial states of this group fulfill the conditions of the model with nonresonance migration of population to higher-angular-momentum Rydberg quasicontinua (Sec. II B). The other group encompasses the initial states $4p(m_0=1)$ and $4s$, the states that fulfill the conditions of the model with resonance migration of the population from the lowest-angular-momentum Rydberg quasicontinuum to the higher-angular-momentum Rydberg quasicontinuum (Sec. II C). For the models with the above initial states, we now present in a graphical form the final results obtained for light of linear polarization and frequency resonant to the $n_0=4\rightarrow n=40$ transition. These results are based on the representative atomic parameters $D_{jj'}$ and Ω_K calculated along the line described in Sec. II A.

A. The $4f(m_0=3)$ and $4d(m_0=2)$ initial-state models

The essence of these models is nonresonance migration of population to higher-angular-momentum Rydberg quasicontinua and in this case we rely on the solution of Sec. II B. In the short-pulse scale, i.e., for pulse durations t shorter than the Kepler period of the band of the excited Rydberg states around $n=40(t\leqslant 2\pi/\Delta=9.7\text{ps})$, the initial state was shown to decay exponentially at the rate R_0 given by Eq. (35). In this case, $1/R_0$ means the initial-state lifetime and in Fig. 3 we show the lifetime of the circular $4f(m_0=3)$ state in its dependence on laser intensity I. At low intensities, the function $\mathrm{Re}G_1(0)$ involved in $1/R_0$ is of the order of 1 and thus the lifetime initially decreases as the inverse of intensity. This is a purely perturbative tendency characterized by the straight line in the log-log plot of Fig. 3. At higher intensities, the effect of $\mathrm{Re}G_1(0)$, i.e., of degenerate Raman couplings in the model consists in changing this tendency, i.e., in increasing the lifetime with increasing intensity up to some asymptotic intensity-independent value. Such a change of the tendency means the high-intensity initial-state stabilization and we see from the figure that the critical intensity for the $4f(m_0=3)$-state stabilization to begin in our model is $I=2.5\times10^{11}\text{W/cm}^2$. It is worth noting that this critical intensity is of the order $I_{\text{at}}/4^8=(3.5\times10^{16}/4^8)\text{W/cm}^2\simeq5.3\times10^{11}\text{W/cm}^2$, i.e., it corresponds to the electric field of the pulse roughly equal to the Coulombic electric field experienced by the initial-state electron from the nucleus in the real hydrogen atom. At this critical intensity the initial-state lifetime drops to its minimum value $(1/R)_{\text{min}}=98$ fs. The corresponding maximum width of the initial state $(2\pi R_{\text{min}})$ appears to be two orders of magnitude smaller than the distance of the initial state from the neighboring state with its principal quantum number equal to 5. Under such a condition the initial state of $n_0=4$ is well isolated from all other states of $n\neq n_0$, as it was required in our model.

Now, we choose appropriately the pulse duration and for the duration chosen we study the effect of laser intensity on the population of different states of the model. We let the initial state $4f(m_0=3)$ survive the pulse assuming the pulse duration not to exceed significantly the minimum lifetime of this state. Precisely, we choose 100-fs pulse duration, nearly corresponding to 0.01 of the Kepler period of the excited Rydberg states around $n=40$, or to 20 optical cycles of the light employed. The spectral width of the pulse of this duration is found to be smaller than the energy gap between the excited Rydberg states around $n=40$ and the ionization threshold. The fulfillment of the condition like that is necessary because no direct one-photon ionization of the initial state is allowed in the model. For the 100-fs pulse duration we show in Fig. 4 the effect of laser intensity on the population of the $4f(m_0=3)$ initial state, the first Rydberg quasicontinum of $l=4$, and the atomic continuum. In the scale of Fig. 4, it was impossible to include the appropriate curves for the higher-angular-momentum Rydberg quasicontinua due to negligible population of these quasicontinua. For example, the maximum population of the second quasicontinuum was calculated to be smaller than that of the first quasicontinuum by as many as four orders of magnitude. It is

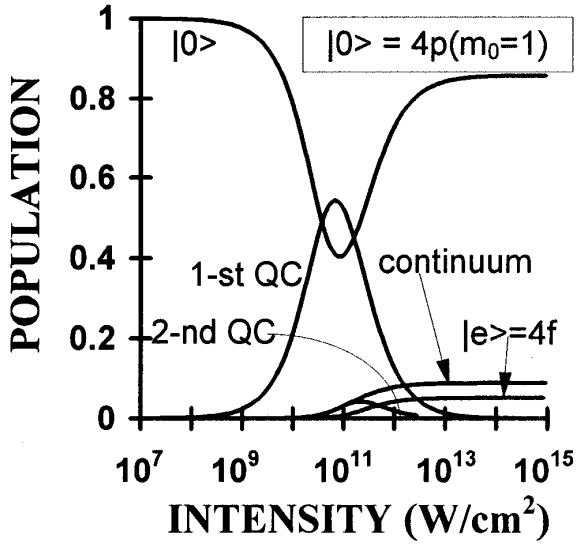

FIG. 5. The population of the initial state $|0\rangle=4p(m_0=1)$, the first and second Rydberg quasicontinua of $l=2$ and 4, respectively, the resonant state $|e\rangle=4f(m=1)$, and the continuum versus laser intensity for a 100-fs laser pulse. The polarization and frequency of light are as in Fig. 3.

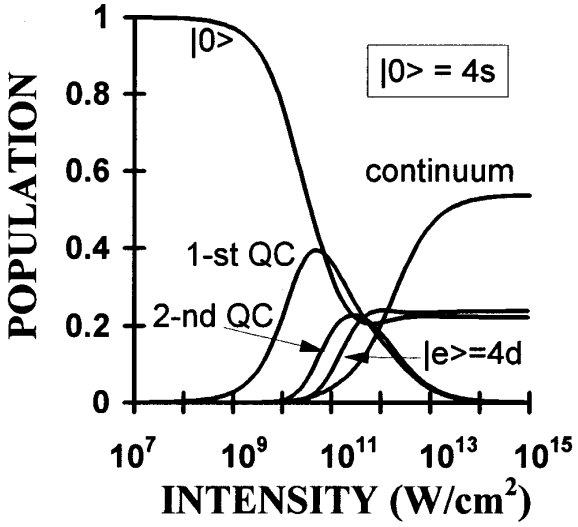

FIG. 6. The population of the initial state $|0\rangle=4s$, the resonant state $|e\rangle=4d(m=0)$, the first and second Rydberg quasicontinua of $l=1$ and 3, respectively, and the continuum versus laser intensity, for a 100-fs laser pulse. The polarization and frequency of light are as in Fig. 3.

thus evident that in the case of the $4f(m_0=3)$ initial state, when no resonance migration of population to higher-angular-momentum Rydberg quasicontinua is possible, the dynamics of the ionization is completely determined by the initial state and the first Rydberg quasicontinuum which is directly coupled to this state. What we see in Fig. 4 is, that in the perturbative regime of low intensities, the initial state is the stronger depleted the higher the intensity and the population removed from this state is transferred mainly to the first quasicontinuum, with only a little population being sent to the continuum. After passing the critical intensity of 2.5×10^{11} W/cm^2 this tendency is reversed. In this strongly nonperturbative regime, the initial state is the weaker depleted the higher the intensity. At the same time, the amount of the population transferred to the first quasicontinuum decreases with increasing intensity down to zero in the high-intensity limit. Consequently, the ionization stabilizes at the level of 0.06 probability when intensity passes the threshold value of about 10^{13} W/cm^2. At this threshold intensity, some amount of population is still kept in the first quasicontinuum, but for intensities well above this threshold the suppression of ionization has its main source in the initial-state survival. Obviously, the level to which the ionization is suppressed depends on the pulse duration and we checked that for the longest pulse allowed by our solution of Sec. II B ($\tau=1$, corresponding to 9.7 ps in the case studied) no high-intensity ionization suppression took place, i.e., the ionization was complete.

For the other initial state $4d(m_0=2)$, we found the results comparable even qualitatively to those shown in Figs. 3 and 4. This is why these additional results are not presented here.

B. The $4p(m_0=1)$ and $4s$ initial-state models

Contrary to the previously considered models, now there is open the resonance channel of population migration from the first to the second Rydberg quasicontinuum through the $4f$ or $4d$ state, respectively. We thus apply the solution of Sec. II C and, assuming the same pulse duration as previously (100 fs), we study the population of different states of the models with resonance migration versus laser intensity. The results for the $4p(m_0=1)$ initial-state model are shown in Fig. 5, whereas those for the $4s$ initial-state model are shown in Fig. 6. It was impossible to show in the scale of these figures the curves relevant for the third and next quasicontinua because the population transferred to them is small. For example, the maximum population reached by the third quasicontinuum turned out to be smaller by three orders of magnitude when compared to the maximum population acquired by the resonantly coupled first and second quasicontinua.

Let us comment on Fig. 5 first. As seen, the curves for the initial state $4p(m_0=1)$, the first Rydberg quasicontinuum of $l=2$, and the continuum look qualitatively the same as the corresponding curves for the model with nonresonance migration (compare with Fig. 4). However, there are two new points. One point is that now the second quasicontinuum is populated as well, mainly at intermediate intensities, with the maximum population being approximately ten times smaller than that of the first quasicontinuum. The other point is that the $4f(m=1)$ state, being the resonant intermediary in the degenerate Raman transition between the first and second Rydberg quasicontinua, also gains population. The population transferred to this resonant state saturates at the level of 0.05. As a result, the observed high-intensity suppression of ionization is now a combined effect of mainly the initial-state survival and the trapping of population in the resonant $|e\rangle$ state. It makes a difference when compared to the model with nonresonance migration. Finally, let us note that the threshold intensity stabilizing the ionization (now at the level of 0.09) is of the same order of magnitude (about 10^{13} W/cm^2) as it was in the previously discussed models

with nonresonance migration (see Fig. 4).

Figure 6, valid for the $4s$ initial-state model, shows results which differ markedly from those in Fig. 5. First of all, the second quasicontinuum is now populated significantly at intermediate intensities (up to 0.22). The next difference is that the initial-state population versus intensity does not show a so well-pronounced minimum and the high-intensity initial-state survival probability is on a much lower level (0.23). Also, the resonant $4d$ state, as the intermediary in the degenerate Raman coupling between the first and second quasicontinua, traps a significant amount of population which at high intensities even exceeds the population survived in the initial state. Finally, the high-intensity ionization is much less suppressed (to 0.53 only) and the threshold stabilizing intensity is now higher by over an order of magnitude (above 10^{14} W/cm^2).

IV. CONCLUSIONS

We have performed model analytical studies of intense-laser ionization from an isolated atomic state via a band of high-Rydberg states, including the possible degenerate Raman migration of population from the directly excited Rydberg states to the Rydberg states of higher angular momentum. Our studies suffer from the approximations of representative n-independent Raman couplings and equal spacing of high-Rydberg states. These two approximations should be removed in the first turn in future more sophisticated studies to make our model atom a better imitation of the real hydrogen atom. We are afraid, however, that without these approximations an analytical solution to the problem will not probably be possible.

The results obtained within our models suggest that an effective migration of population from lower- to higher-angular-momentum Rydberg states of $n \gg 1$ due to degenerate Raman coupling is likely to occur only if the Raman process is resonant. Whether it is resonant or not depends on the choice of the initial state. We believe that the population transferred resonantly to a band of higher-angular-momentum Rydberg states could be detected in an experiment consisting in measuring the photoelectron angular distributions versus laser intensity. At the intensity ensuring efficient migration, the spherical harmonic of the angular-momentum quantum number higher by 2 than the number determined by the directly excited first Rydberg quasicontinuum is expected to contribute substantially to the distributions. Our conclusion on the migration coincides with that derived by Grobe, Leuchs, and Rzażewski [11] from their related model in which the population was considered to migrate from the initially prepared $28s$ state in hydrogen to higher-l states of the same principal quantum number under the action of laser pulse of quite different time and intensity parameters.

Since the nonresonance Raman migration of population to higher-l Rydberg states appeared to be very weak in our model, we found no evidence that it affects stabilization. In this case, the bound-state subspace which plays the dominant role in the ionization process is formed by the initial state and the Rydberg states directly coupled to it. The degenerate Raman redistribution of the population between the directly excited Rydberg states of the same l but different n, pointed out by Fedorov and co-workers [16], is in this case important for stabilization to appear (see also [6,7,9,10]). In our model with no resonance migration to higher-l states, we found the initial-state survival as the main cause of the high-intensity stabilization, with only a small effect of trapping of population in high-Rydberg states.

In the case when the population from the directly excited Rydberg states could migrate resonantly to higher-l Rydberg states through a state orbitally degenerate with the initial one, a different cause of stabilization was found. Mainly, it was the combination of the initial-state survival with the trapping of population in the resonant state being the intermediary in the Raman transition between Rydberg states differing by 2 in the orbital quantum number. A significant amount of the population was found to be trapped in the resonant state at high intensities. In the case when the channel of resonance migration of population between different-l high-Rydberg states was opened, a profound effect of the initial-state orbital quantum number on redistribution of population by laser pulse, stabilizing intensities, and the level of stabilization was found.

For a 100-fs pulse assumed by us, the threshold intensities stabilizing our model atom against ionization via high-Rydberg states were found to be at the level of 10^{13} W/cm^2 at the optimum choice of the initial state. This threshold intensity is of the same order as that observed experimentally by de Boer *et al.* [2] for a quite different process, namely, the high-frequency stabilization of the circular $5g$ state in neon.

ACKNOWLEDGMENTS

One of us (A.W.) would like to thank the Polish Committee for Scientific Research for the support under Grant No. 2 PO 3B 188 10.

[1] K. Burnett, V. C. Reed, and P. L. Knight, J. Phys. B **26**, 561, 1993 (see for review and references).

[2] M. P. de Boer, J. H. Hoogenraad, R. B. Vrijen, R. C. Constantinescu, L. D. Noordam, and H. G. Muller, Phys. Rev. A **50**, 4085 (1994).

[3] M. Pont and M. Gavrila, Phys. Rev. Lett. **65**, 2362 (1990); R. J. Vos and M. Gavrila, *ibid.* **68**, 170 (1992).

[4] R. M. Potvliege and H. G. Smith, Phys. Rev. A **48**, R46 (1993).

[5] Q. Su, J. H. Eberly, and J. Javanainen, Phys. Rev. Lett. **64**, 862 (1990).

[6] B. Piraux, E. Huens, and P. L. Knight, Phys. Rev. A **44**, 721 (1991).

[7] E. Huens and B. Piraux, Phys. Rev. A **47**, 1568 (1993).

[8] F. H. M. Faisal and L. Dimou, Acta Phys. Pol. **86**, 201 (1994).
[9] M. Yu Ivanov, Phys. Rev. A **49**, 1165 (1994).
[10] A. Wójcik and R. Parzyński, Phys. Rev. A **51**, 3154 (1995).
[11] R. Grobe, G. Leuchs, and K. Rzażewski, Phys. Rev. A **34**, 1188 (1986).
[12] Z. Deng and J. H. Eberly, J. Opt. Soc. Am. B **2**, 486 (1985); J. Phys. B **18**, L287 (1985); also J. H. Eberly, J. Javanainen and K. Rzażewski, Phys. Rep. **204**, 331 (1991).
[13] W. I. Ritus, Zh. Éksp. Teor. Fiz. **51**, 1544 (1966).
[14] P. Avan, C. Cohen-Tannoudji, J. Dupont-Roc, and C. Fabre, J. Phys. (Paris) **37**, 993 (1976).
[15] G. Feldman, T. Fulton, and B. R. Judd, Phys. Rev. A **51**, 2762 (1995).
[16] M. V. Fedorov, Laser Phys. **3**, 219 (1993); M. V. Fedorov, M. Yu Ivanov, and P. B. Lerner, J. Phys. B **23**, 2505 (1990); M. V. Fedorov, M. Yu Ivanov, and A. M. Movsesian, *ibid.* **23**, 2245 (1990); M. V. Fedorov and A. M. Movsesian, J. Opt. Soc. Am. B **6**, 928 (1989).
[17] G. C. Stey and W. Gibberd, Physica **60**, 1 (1972).